The study of X-ray *M*-shell spectra of W ions from the Lawrence Livermore National Laboratory Electron Beam Ion Trap

P. Neill, C. Harris, A.S. Safronova, S. Hamasha, S. Hansen, U.I. Safronova, and P. Beiersdorfer

Abstract: *M*-shell spectra of W ions have been produced at the Lawrence Livermore National Laboratory EBIT-II electron beam ion trap-II at different energies of the electron beam. A survey has been performed at 2.4, 2.8, and 3.6 keV, and for steps in energy of 100 eV over the 3.9–4.6 keV energy range. The analysis of 11 W spectra has shown the presence of a wide variety of ionization stages from Se-like to Cr-like W; the appearances of these ionization stages correlate well with the energy of their production. The present paper focuses on the identification of 63 experimental features of W ions in a spectral region from 5 to 6 Å (1 Å = 10^{-10} m) using calculations with inclusion of all ionization stages matching this spectral region. The majority of lines in all spectra have been identified and assigned to the $4f \rightarrow 3d$ and $4d \rightarrow 3p$ transitions. This is the first work that lists a comprehensive identification of so many resolved spectral features of X-ray *M*-shell transitions in W ions recorded in such detail in the laboratory.

PACS Nos.: 52.58.Lq,32.30.Rj,52.70.La

Résumé : Nous avons produit des spectres dans la couche *M* d'ions W à l'aide du faisceau d'électrons du EBIT-II du Lawrence Livermore National Laboratory à différentes énergies du faisceau. L'étude a été faite à 2.4, 2.8 et 3.6 keV et entre 3.9 et 4.6 keV avec des sauts de 100 eV. L'analyse de 11 spectres de W a montré la présence d'une large variété de seuils d'ionisation, allant du W de type Se au type Cr. L'apparition de ces seuils d'ionisation est en bonne corrélation avec leur énergie de production. Nous identifions 63 caractéristiques expérimentales des ions W dans la région spectrale entre 5 et 6 Å (1 Å = 10^{-10} m) en utilisant des calculs incluant tous les seuils d'ionisation correspondant à cette région spectrale.. La majorité des lignes de tous les spectres ont été identifiées et assignées aux transitions $4f \rightarrow 3d$ et $4d \rightarrow 3p$. Ceci est le premier travail qui présente une liste aussi complète d'un aussi grand nombre de caractéristiques-X identifiées dans la couche *M* d'ions W et mesurées avec autant de précision en laboratoire.

[Traduit par la Rédaction]

Received 5 March 2004. Accepted 16 August 2004. Published on the NRC Research Press Web site at http://cjp.nrc.ca/ on 20 November 2004.

P. Neill, C. Harris, A.S. Safronova,[1] S. Hamasha, S. Hansen, and U.I. Safronova. Physics Department/220, University of Nevada, Reno, NV 89557, USA.
P. Beiersdorfer. Lawrence Livermore National Laboratory, Livermore, CA 94550, USA.

[1]Corresponding author (e-mail: alla@physics.unr.edu).

Fig. 1. Experimental M-shell spectra of W ions produced at the energies of the electron beam of 2.4, 2.8, 3.6, and 3.9 keV. Intense spectral features are identified with a certain W ion and a certain group of transitions (see text).

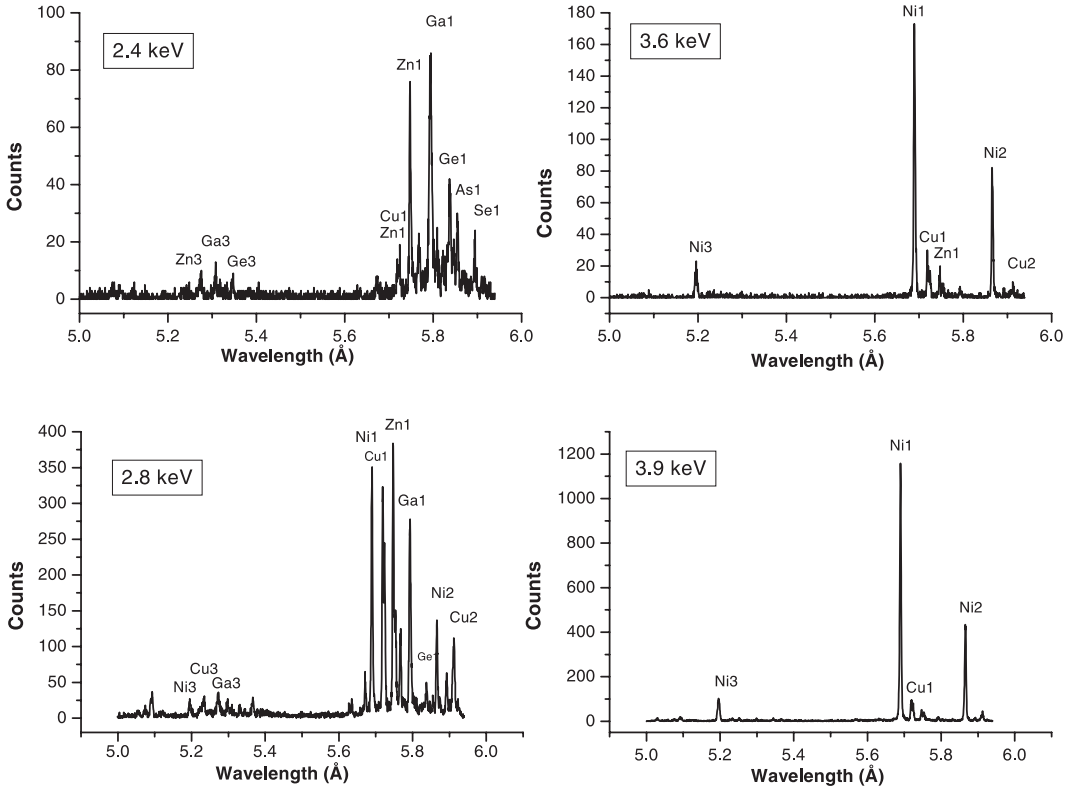

1. Introduction

Tungsten (W) wire explosions are studied very intensively at Sandia National Laboratories. Results of tungsten wire-array Z-pinch experiments and modeling have been published elsewhere [1,2]. High-resolution X-ray spectral data have been accumulated in tungsten experiments on Z [3], which require a development of appropriate theoretical modeling. The study of X-ray M-shell spectra of W ions produced by high-temperature plasmas is a very complicated problem because of the simultaneous contributions from numerous ionization stages. For example, the majority of line emissions in the spectral region from 5 to 6 Å (1 Å $= 10^{-10}$ m) are composed of hundreds of $4l' \rightarrow 3l$ transitions and more than ten ionization stages. Identification of this spectral region is a complex problem even for low-density tokamak plasmas [4]. To the best of our knowledge, the first X-ray M-shell spectra of W were produced by high-density exploded-wire plasmas more than 25 years ago. The precision of the measurement of the transitions energies achieved at the ± 10 eV level was sufficient to identify three Ni-like W lines and determine ionization states from Zn-like to Fe-like W, but was not enough for the purely spectroscopic tabulations [5]. The precision of the measurement of the $4l' \rightarrow 3l$ Ni-like W transitions was substantially improved three years later in the identification of Hf XLV, Ta XLVI, W XLVII, and Re XLVIII ions produced by laser plasmas [6]. The following paper on laser plasma M-shell heavy ions [7] concentrated on $4p \rightarrow 3d$ transitions in Co- and Cu-like W and Tm because their separation is greater than for the $4f \rightarrow 3d$ spectral lines. The extended analysis of the X-ray spectra of laser-irradiated W included $nf \rightarrow 3d$ ($n = 5$ through 9), $nd \rightarrow 3p$ ($n = 4$ through 6), and

Fig. 2. Experimental M-shell spectra of W ions produced at the energies of the electron beam of 4.0, 4.1, 4.2, 4.3, and 4.4 keV. Intense spectral features are identified with a certain W ion and a certain group of transitions (see text).

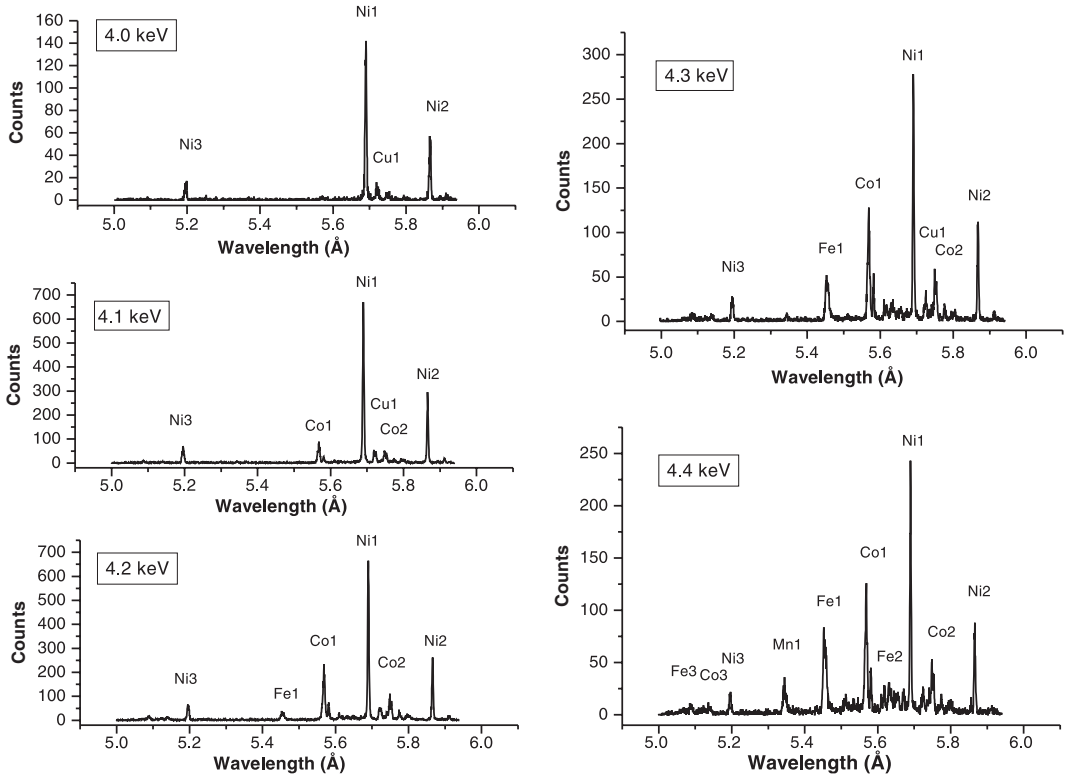

$np \rightarrow 3s$ ($n = 4, 5$) transitions [8].

Recently, electron-beam ion-trap EUV spectra of W ions have been studied at the Berlin [9] and Livermore [10] electron-beam ion traps. In electron-beam ion-trap experiments, the complicated M-shell spectrum can be decomposed in various spectra formed by the contribution of only a few ionization stages allowing for the possibility of unravelling the tungsten M-shell emission. These capabilities have been used to identify the complex extreme ultra-violet (EUV) emission [9, 10] and X-ray emission of W in the this paper. Specifically, we present an analysis of 11 X-ray M-shell spectra produced at different energies of the electron beam. These spectra are formed by a wide variety of ionization stages of W ions, from Se- to Cr-like W. The important feature of these spectra is that every spectrum includes prominent lines from only a few ionization stages. The variation in intensities with beam energy allows these lines to be uniquely identified with particular charge states. Some atomic data and spectral intensities for Co-like to Rb-like W ions have been calculated previously for a high-temperature, low-density plasma in a broad spectral range $0 < \lambda < 20$ Å [11]. In the present paper, we focus on the identification of the experimental spectral features of W ions in a spectral range from 5 to 6 Å using the calculations that include all ionization states matching this spectral region.

2. Experimental *M*-shell spectra in the spectral region from 5 to 6 Å

An M-shell survey of W ions was performed at the Lawrence Livermore National Laboratory using the EBIT-II electron-beam ion trap [12]. The trapped W ions reach a charge-state limit when the electron

Fig. 3. Experimental M-shell spectra of W ions produced at the energies of the electron beam of 4.5 and 4.6 keV. Intense spectral features are identified with a certain W ion and a certain group of transitions (see text).

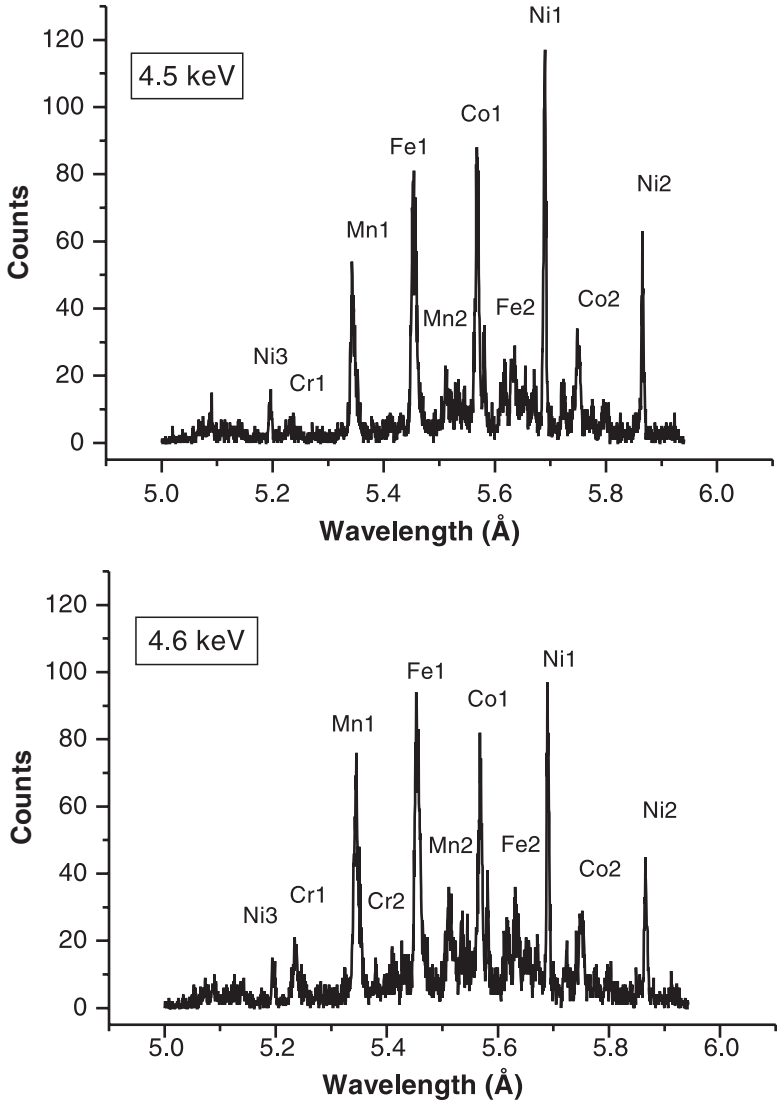

beam energy is below the energy required to produce the next higher charge state. For this survey, steady-state electron beam energies were 2.4, 2.8, 3.6 keV, and in steps of 100 eV over the 3.9–4.6 keV energy range. The 11 experimental spectra, shown in Figs. 1–3, are each dominated by one or a few charge states, and exhibit the shift in charge balance toward higher charge states with increasing beam energy. These spectra were recorded by a wide-band, high-resolution soft X-ray spectrometer [13] with a PET(002) crystal. The resolution was $\lambda/\Delta\lambda = 2200$ and the detected spectral range was from 5 to 5.94 Å .

Two prominent phosphorus lines, Ly_α ($\lambda = 5.3814$ Å) and the He-like resonance line w ($\lambda = 5.7600$ Å), were used directly for wavelength calibration of the spectra taken at 2.4 and 3.9 keV. The wavelength scale was determined using a Gaussian profile fitting function followed by a correction to account for the intersection of the dispersion plane with the flat face of the position-sensitive proportional

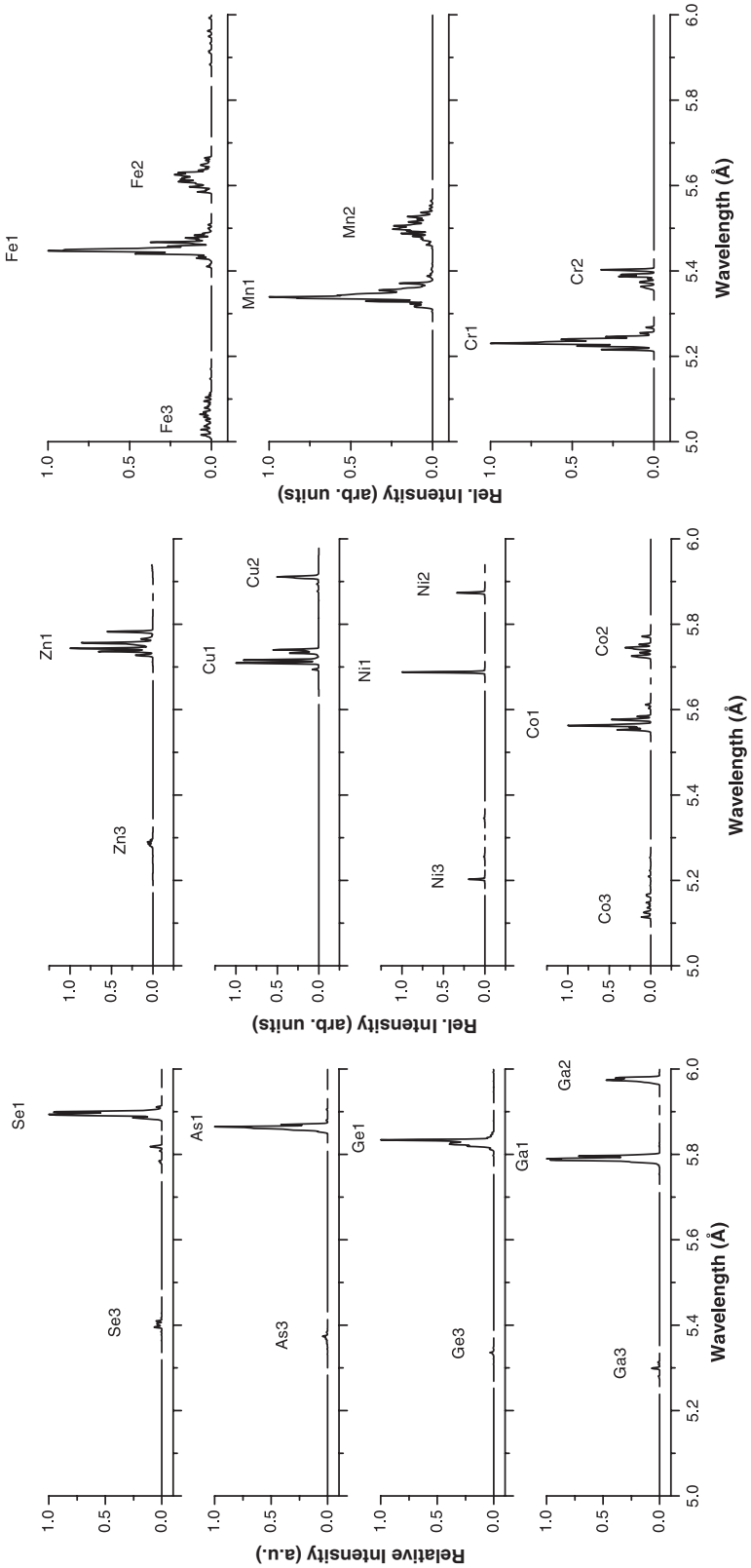

Fig. 4. Theoretical synthetic spectra of Se- to Cr-like W ions calculated using a kinetic code.

Fig. 5. (*a*) Comparison of the experimental spectrum (black) produced at 2.4 keV with the synthetic spectrum (red) of Ga-like W. (*b*) Comparison of the experimental spectrum (black) produced at 4.6 keV with the synthetic spectrum (red) of Fe-like W.

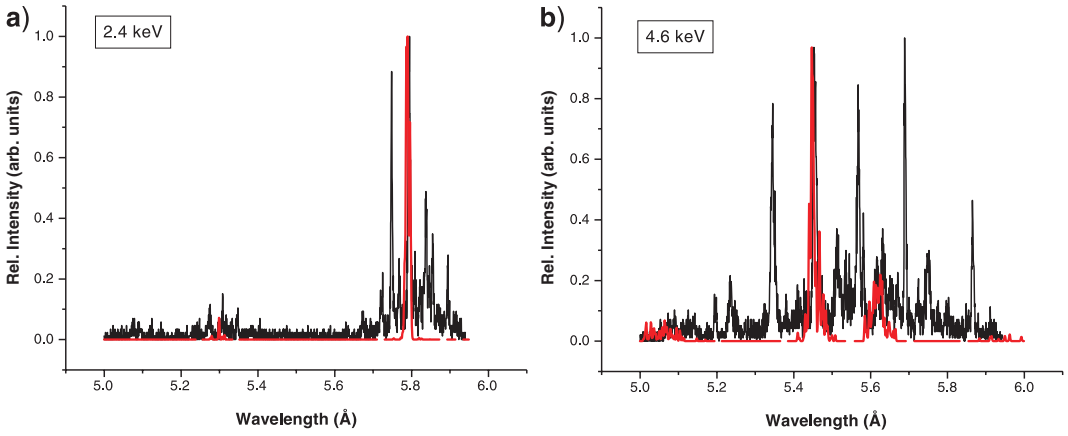

Table 1. Wavelengths (λ in Å) and weighted transition rates (gA_r in s^{-1}) in Ni-like W for transitions from odd-parity states with $J = 1$ to the ground state. Theoretical data obtained using RMBPT and Cowan codes are compared with various experimental results. The numbers in brackets represent powers of 10.

		Experiment		Theory			
jj label	*LS* label	λ_{exp}	λ_{exp}	λ_{RMBPT}	λ_{COWAN}	gA_r^{RMBPT}	gA_r^{COWAN}
$3d_{3/2}4p_{1/2}(1)$	$3d4p\ ^3D_1$		7.170[b]	7.174	7.164	2.01[13]	1.62[13]
$3d_{5/2}4p_{3/2}(1)$	$3d4p\ ^1P_1$		7.024[b]	7.027	7.008	3.83[13]	3.91[13]
$3d_{3/2}4p_{3/2}(1)$	$3d4p\ ^3P_1$		6.775[b]	6.778	6.754	4.26[12]	5.35[12]
$3p_{3/2}4s_{1/2}(1)$	$3p4s\ ^1P_1$		6.154[b]	6.154	6.174	6.65[13]	5.21[13]
$3d_{5/2}4f_{5/2}(1)$	$3d4f\ ^3P_1$		5.956[b]	5.953	5.946	7.24[11]	3.90[11]
$3d_{5/2}4f_{7/2}(1)$	$3d4f\ ^3D_1$	5.8665[a]	5.871[b]	5.870	5.868	3.54[14]	4.21[14]
$3d_{3/2}4f_{5/2}(1)$	$3d4f\ ^1P_1$	5.6900[a]	5.689[b]	5.689	5.685	1.12[15]	1.22[15]
$3p_{1/2}4s_{1/2}(1)$	$3p4s\ ^3P_1$			5.345	5.324	1.71[13]	3.05[13]
$3p_{3/2}4d_{3/2}(1)$	$3p4d\ ^3P_1$	5.2509[a]	5.255[c]	5.255	5.272	1.58[13]	1.77[13]
$3p_{3/2}4d_{5/2}(1)$	$3p4d\ ^1P_1$	5.1963[a]	5.203[c]	5.201	5.218	2.82[14]	2.55[14]

[a] Experimental results of the present paper.
[b] Experimental results from ref. 6.
[c] Experimental results from ref. 8

counter. As noted in previous measurements utilizing similar detectors [14], the line positions at the single-wire proportional counter were observed to shift physically by small amounts from one spectrum to the next. There were two components to these small shifts. The most pronounced was a seemingly random systematic shift of the entire spectrum toward higher or lower detector channels. Smaller random shifts displaced individual lines relative to the others. The systematic shifts may have been caused by mechanical vibration or thermal expansion and contraction of the spectrometer, but these mechanisms fail to explain the random line-to-line shifts within spectra. As there was about 1 mÅ of systematic shift from spectrum to spectrum, we used the prominent Ni-like Ni1 and Ni2 lines as a secondary standard. These Ni-like lines are present in all the spectra except those taken at a beam energy of 2.4 keV, and were used to calibrate the wavelength scale for the 2.8–4.6 keV spectra. The line-to-line random shifts are responsible for a relative wavelength uncertainty of 0.3 mÅ .

Table 2. Identification of lines in M-shell spectra of W produced at different energies of the electron beam from 2.4 to 3.6 keV.

		λ			
N	Ion		Expt. (keV)		
Group		Theor.	2.4	2.8	3.6
7	Ni3	5.201[a]		5.1953	5.1976
8	Cu3	5.230		5.2239	
9	Cu3	5.241		5.2331	
11	Ni3	5.255[a]		5.2491	
12	Zn3	5.280	5.2738	5.2705	
13	Ga3	5.300	5.3081	5.2977	
14	Ge3	5.321		5.3142	
16	Ge3	5.336		5.3311	
18	Ge3	5.348	5.3465	5.3448	
22	Se3	5.395		5.3933	
24	Se3	5.410		5.403	
46	Ni1	5.689[a]		5.690	5.690
47	Cu1	5.716	5.7193	5.719	5.7189
48	Cu1	5.723	5.7242	5.724	5.724
49	Zn1	5.748	5.7477	5.7473	5.747
52	Zn1	5.756	5.7541	5.7534	5.7538
53	Zn1	5.765	5.7678	5.7671	
55	Ga1	5.788	5.7922	5.7925	5.7924
56	Ga1	5.791	5.7950	5.7952	
57	Ge1	5.821	5.8315	5.8299	
58	Ge1	5.827	5.8378	5.8377	
59	Ge1	5.836	5.8465	5.8467	
60	As1	5.862	5.8552	5.855	
61	Ni2	5.870[a]		5.867	5.867
62	Se1	5.894	5.894	5.8927	
63	Cu2	5.905	5.9169	5.9129	5.9128

Atomic data calculated using the Cowan code.
[a] Atomic data calculated using RMBPT code.

The 11 experimental spectra were accumulated for varying periods, so intensity comparisons between spectra are not meaningful. Line intensity as shown in the figures is measured in counts and no intensity correction was made for polarization effects of the crystal or for the response function of the 1 μm Lexan window of the wide-band spectrometer.

All together, we have studied 11 spectra recorded in the spectral region from 5 to 6 Å , which are presented in Figs. 1–3. The observed transitions are $4l' \rightarrow 3l$ transitions from Se-like through Cr-like W. For all 11 spectra the brightest lines are lines due to $4f_{5/2} \rightarrow 3d_{3/2}$ transitions (Group 1). The most prominent lines in the majority of spectra are Ni-like ion lines. Group 2 is made up of $4f_{7/2} \rightarrow 3d_{5/2}$ transitions, these are less intense and have longer wavelengths than Group 1. Group 3, formed by $4d \rightarrow 3p$ transitions, is characterized by less intense lines with shorter wavelengths than Groups 1 and 2. Ga-like lines from Group 1 (Ga1) dominate the 2.4 keV spectrum, whereas a Ni-like line (Ni1) dominates in the other ten spectra. The most intense of the Cu-like line peaks (Cu1) are observed in all spectra. Zn-like line features are very intense in the 2.4 keV spectra, then decrease in relative intensities through the 4.0 keV spectrum. Co-like lines appear in the 3.9 keV spectrum and are very intense in 4.2–4.6 keV spectra. Mn-like and Fe-like line features became very prominent in 4.5 and 4.6 keV spectra.

Table 3. Identification of lines in M-shell spectra of W produced at different energies of the electron beam from 3.9 to 4.1 keV.

		λ			
N	Ion		Expt. (keV)		
Group		Theor.	3.9	4.0	4.1
7	Ni3	5.201[a]	5.1944	5.1974	5.1969
8	Cu3	5.230	5.2264		5.2259
9	Cu3	5.241	5.2338		
11	Ni3	5.255[a]	5.2518	5.2514	5.2511
12	Zn3	5.280	5.2727		
13	Ga3	5.300	5.2988		
14	Ge3	5.321	5.3126		
24	Se3	5.410	5.4053		
36	Co1	5.558			5.5646
37	Co1	5.563	5.5684	5.5705	5.5688
39	Co1	5.577	5.5812		5.5808
41	Fe2	5.608	5.6101		
43	Fe2	5.626	5.6277		
44	Fe2	5.630	5.6355		
46	Ni1	5.689[a]	5.690	5.690 6	5.690
47	Cu1	5.716	5.7189	5.7184	5.7186
48	Cu1	5.723	5.7241	5.724	5.7238
49	Zn1	5.748	5.7467	5.7467	
50	Co2	5.745			5.7476
51	Co2	5.753			5.7531
52	Zn1	5.756	5.7535	5.7534	
53	Zn1	5.765	5.7678		
54	Co2	5.774			5.7743
55	Ga1	5.790	5.7933	5.7935	
61	Ni2	5.870[a]	5.866	5.866	5.866
62	Se1	5.894	5.8921	5.8943	5.8924
63	Cu2	5.905	5.9127	5.9105	5.9125

Atomic data calculated using the Cowan code.
[a] Atomic data calculated using RMBPT code.

3. Modeling of *M*-shell W spectra in the spectral region from 5 to 6 Å

To identify the X-ray M-shell spectra of W ions, the necessary atomic data have been calculated and the collisional-radiative atomic kinetic model has been developed. Atomic data of all needed isoelectronic sequences matching this spectrum were calculated using the Multiconfigurational Hartree–Fock (MCHF) code developed by Cowan [15]. Also, wavelengths and transition probabilities for Ni-like W lines were calculated using the fully relativistic many-body code (RMBPT code) [16]. Table 1 presents wavelengths and transition rates for transitions from ten excited $J = 1$ states to the ground state in Ni-like W. Theoretical data obtained by using RMBPT and Cowan codes are compared with experimental spectra of this paper and the previous experimental work published in refs. 6 and 8. The accuracy of the measured wavelengths was 5 mÅ in ref. 6 and 2 mÅ in ref. 8. The experimental wavelengths of four Ni-like lines (7, 11, 46, and 61) from this paper are averaged values over all measurements listed in Tables 2–4.

The second-order RMBPT calculations implemented here for Ni-like ions start from a $1s^2 2s^2 2p^6 3s^2 3p^6 3d^{10}$ Dirac–Fock potential [16]. All possible $3l$ holes and $4l$ particles forming 56

Table 4. Identification of lines in *M*-shell spectra of W produced at different energies of the electron beam from 4.2 to 4.6 keV.

		λ					λ			
N	Ion	Theor.	Exp. (keV)		N	Ion	Theor.	Exp. (keV)		
Group			4.2	4.3	Group			4.4	4.5	4.6
2	Fe3	5.081		5.0842	1	Fe3	5.065	5.0677	5.0696	
3	Fe3	5.096	5.0901		2	Fe3	5.081	5.0857	5.089	5.088
4	Co3	5.114	5.1089		3	Fe3	5.096	5.0902		
5	Co3	5.124	5.1211	5.1219	4	Co3	5.114		5.1106	
6	Co3	5.136	5.1375	5.1379	5	Co3	5.124	5.1232		5.1257
7	Ni3	5.201[a]	5.1978	5.1962	6	Co3	5.136	5.1393	5.1389	
8	Cu3	5.230	5.2269		7	Ni3	5.201[a]	5.1959	5.1959	5.1960
9	Cu3	5.241	5.2382		10	Cr1	5.238		5.2371	5.236
11	Ni3	5.255[a]	5.2512		15	Mn1	5.324		5.3239	5.3236
19	Mn1	5.339	5.3443	5.344	17	Mn1	5.335	5.3416	5.3427	5.3406
25	Fe1	5.441	5.4495		19	Mn1	5.339	5.345	5.3467	5.3448
26	Fe1	5.447	5.4532	5.4513	20	Mn1	5.345	5.3496	5.3526	5.3508
27	Fe1	5.451	5.4581	5.4551	21	Cr2	5.387		5.3799	5.3801
28	Fe1	5.458		5.4584	23	Cr2	5.403		5.3992	5.3997
29	Fe1	5.467	5.4632	5.4632	25	Fe1	5.441	5.4486	5.449	
30	Fe1	5.477		5.471	26	Fe1	5.447	5.4521	5.4526	5.452
32	Mn2	5.505	5.5114	5.5103	27	Fe1	5.451	5.456	5.4577	5.4563
34	Mn2	5.527		5.535	28	Fe1	5.458	5.4595		
36	Co1	5.558	5.5639	5.5647	29	Fe1	5.467	5.4644	5.4646	5.4667
37	Co1	5.563	5.5681	5.5686	30	Fe1	5.477	5.4688	5.4715	5.4726
38	Co1	5.566	5.5708	5.5721	31	Mn2	5.494	5.5063	5.504	5.505
39	Co1	5.577	5.5809	5.5815	32	Mn2	5.505	5.5124	5.512	5.511
41	Fe2	5.609	5.6099	5.6107	33	Mn2	5.522	5.5277	5.5281	
42	Fe2	5.615	5.6183	5.6181	34	Mn2	5.527	5.534	5.5346	5.5339
43	Fe2	5.626	5.6284	5.6299	35	Mn2	5.537	5.5455	5.5443	5.5458
44	Fe2	5.630	5.633	5.6345	36	Co1	5.558	5.5646	5.5634	5.5635
45	Fe2	5.636	5.6379	5.639	37	Co1	5.563	5.5682	5.5677	5.5683
46	Ni1	5.689[a]	5.690	5.691	38	Co1	5.566	5.5714	5.5713	5.5709
47	Cu1	5.716	5.7194	5.720	39	Co1	5.577	5.5811	5.5809	5.5815
48	Co2	5.726	5.724	5.7246	40	Fe2	5.597	5.5934	5.5949	5.5977
50	Co2	5.745	5.7479	5.7492	41	Fe2	5.609	5.6107	5.6105	5.6104
51	Co2	5.753	5.7529	5.754	42	Fe2	5.615	5.618	5.6168	5.6174
54	Co2	5.774	5.7741	5.776	43	Fe2	5.626	5.6297	5.6297	5.6305
61	Ni2	5.870[a]	5.866	5.868	44	Fe2	5.630	5.6335	5.6351	5.6361
62	Se1	5.894	5.8917		45	Fe2	5.636	5.6375		5.6395
63	Cu2	5.905	5.9116	5.9128	46	Ni1	5.689[a]	5.690	5.690	5.690
					47	Cu1	5.716	5.719	5.7202	
					48	Co2	5.726	5.7242	5.7251	5.7234
					50	Co2	5.745	5.7483	5.748	5.7479
					51	Co2	5.753	5.7534	5.7526	5.7534
					54	Co2	5.774	5.7744	5.7747	5.7746
					61	Ni2	5.870[a]	5.867	5.866	5.866
					63	Cu2	5.905	5.9117		

Atomic data calculated using the Cowan code.

[a] Atomic data calculated using RMBPT code.

odd-parity and 50 even-parity $3l_j4l'_{j'}$ (J) states have been considered. In general, theoretical results are in a good agreement with experiment, however, RMBPT wavelengths agree much better with experimental measurements than Cowan wavelengths because of the fully relativistic approach. For example, for the transitions from the $3p_{3/2}4d_{5/2}$ (1) and $3p_{3/2}4d_{3/2}$ (1) levels, RMBPT calculations give $\lambda_{\mathrm{RMBPT}} = 5.201$ Å and $\lambda_{\mathrm{RMBPT}} = 5.255$ Å what is much closer to the experimental measurements λ_{exp}=5.1963 Å and $\lambda_{\mathrm{exp}} = 5.2509$ Å than Cowan calculations ($\lambda_{\mathrm{COWAN}} = 5.218$ Å and $\lambda_{\mathrm{COWAN}} = 5.272$ Å), respectively. On the other hand, it should be noted that the atomic structure Cowan code produces results that are generally in good agreement with experimental energies by scaling the electrostatic Slater parameters to include the correlation effects. The scaling factor of 0.85 and LS coupling were employed in the Cowan code calculations. Also, contributions from many configurations for each isoelectronic sequence were taken into account in calculations of atomic characteristics by the Cowan code. For example, for Cu-like ions, 14 even- and 12 odd-parity configurations of singly- and doubly-excited states were included in the calculations. To calculate the synthetic M-shell spectra of W, the most intense 542 lines of Cr-like, 345 lines of Mn-like, 461 lines of Fe-like, 148 lines of Co-like, 47 lines of Ni-like, 368 lines of Cu-like, 1213 lines of Zn-like, 522 lines of Ga-like, 370 lines of Ge-like, 147 lines of As-like, and 100 lines of Se-like W ions were included.

A collisional-radiative atomic kinetic model has been developed that includes the ground states of every ionization stage of W from the bare ion with no electrons to neutral W with 74 electrons. Ionization potentials were taken from tables published in refs. 11 and 17. Detailed atomic structure is included for ionization stages from Cr-like to Se-like W. Each fine-structure state is linked to other states within its ionization stage via collisional excitation, collisional de-excitation, and radiative decay. All the states of the ions are linked via collisional ionization, three-body recombination, and radiative recombination. The modified Van Regemorter [18] formula is used to calculate the excitation cross sections of optically allowed transitions. A modified Lotz formula [19] is employed to calculate collisional ionization cross sections. Radiative recombination cross sections are calculated by Kramer's approximation [20]. The electron distribution function had a Gaussian form centered at the energy indicated by an electron beam with a FWHM = 50 eV in agreement with typical distributions measured on EBIT-II [21].

Synthetic spectra of Se- to Cr-like W ions calculated using the kinetic model with lines broadened with Doppler profiles for each of the 11 ionization stages are shown in Fig. 4. The spectra of Se- to Ge-like W exhibit only Group 1 peaks, whereas the spectrum of Ga-like W ions shows peaks corresponding to Groups 1–3. The spectra of Ni- to Co-like W ions consist of peaks due to Groups 1–3. The spectrum of Fe-like W ions also consists of peaks due to Groups 1–3, whereas the spectra from Mn- and Cr-like W ions include two peaks due to Groups 1 and 2.

To identify experimental line features, the wavelengths and intensities of the most intense peaks within the three groups of transitions for each ionization stage were compared with experimental wavelengths and relative intensities. Tables 2–4 list identification of 63 M-shell line features from 11 spectra of W ions. In general, experimental observations agree well with theoretical predictions from this paper and from ref. 11. Specifically, the spectra produced at 2.4 and 2.8 keV (Fig. 1) are rich with ions of ionization stages lower than Ni-like: from Se-like to Cu-like W. The spectrum produced at 2.4 keV is the only spectrum among the 11 spectra where no Ni-like ion lines are observed. The synthetic spectrum of Ga-like W reproduces the most intense lines for this spectral feature and beam energy well (Fig. 5). The spectra produced at 3.6 and 3.9 keV (Fig. 1) and at 4.0, 4.1, and 4.2 keV (Fig. 2) are dominated by Ni-like W lines. In the spectrum produced at 3.6 keV, we still observe the lower ionization stages of Cu- and Zn-like W, whereas in the spectra produced at 4.1–4.2 keV the ionization stages higher than Ni-like, specifically, Co-like W, appear. This correlates well with the jump in the ionization potential from 2430 eV (for Cu-like W) to 4065 eV (for Ni-like W) and explains why the spectra produced at 3.6–4.2 keV include the least number of lines from all spectra considered. The spectra produced at 4.3–4.6 keV (Figs. 2–3) are rich with higher than Ni-like ionization stages: Co-like, Fe-like, Mn-like, and Cr-like W. The spectrum produced at the highest energy, 4.6 keV, includes the most lines. Also, the

maximum number of identified line peaks within a given isoelectronic sequence is 15 for Fe-like W. The synthetic spectrum of Fe-like W reproduces the most relevant spectral features in Fig. 5 well.

4. Conclusion

The survey of 11 W spectra has shown the presence of a wide variety of ionization stages from Se-like to Cr-like W: the appearance of these ionization stages correlates well with the energy of their production. The majority of lines in all spectra have been identified and assigned to the $4f \rightarrow 3d$ and the $4d \rightarrow 3p$ transitions. The Ni-like ions dominate in most spectra. The high resolution of these spectra and the ability to create only a few ionization stages during the spectrum production allows us to perform an excellent analysis of the M-shell spectra that cannot be done with sources other than EBIT. The synthetic spectra calculated using a developed kinetic model reproduce the most intense spectral features in all 11 experimental spectra well.

This work lists for the first time a comprehensive identification of many resolved X-ray spectral features of the M-shell transitions of W recorded in great detail in the laboratory.

This study is very important in the development of M-shell diagnostics of high-density high-temperature Z-pinch plasmas, for example, plasmas of tungsten wire explosions and X-pinches. M-shell spectra of such plasmas include simultaneous contributions from numerous ionization states. Also, if time and spatial integration are employed to collect the spectra, then these, in addition, will complicate the analysis. Nevertheless, the kinetic model used in this paper predicts that the most intense spectral features in z-pinch plasmas are the Ni-, Cu-, and Co-like W features studied in detail in this work.

Acknowledgments

This work was supported by the Department of Energy, National Nuclear Security Agency under University of Nevada, Reno grant DE-FC52-01NV14050 and the Lawrence Livermore National Laboratory under contract No. B520743. Work at the Lawrence Livermore National Laboratory was performed under the auspices of the US Department of Energy under Contract No. W-7405-Eng-48.

References

1. R.B. Spielman, C. Deeney, G.A Chandler, M.R. Douglas, D.L. Fehl, M.K. Matzen, D.H. McDaniel, T.J. Nash, J.L. Porter, T.W.L. Sanford, J.F. Seemen, and W.A. Stygar. Phys. Plas. **5**, 2105 (1998).
2. C. Deeney, C.A. Coverdale, M.R. Douglas, K.W. Struve, R.B. Spielman, W.A. Stygar, D.L. Peterson, N.F. Roderick, M.G. Haines, F.N. Beg, and J. Ruiz-Camacho. Phys. Plas. **6**, 3576 (1999).
3. J.E. Bailey, D. Cohen, G.A. Chandler, M.E. Cuneo, M.E. Foord, R.F. Heeter, D. Jobe, P. Lake, D.A. Liedahl, J.J. MacFarlane, T.J. Nash, and D. Nielson. J. Quantum. Spectrosc. Radiat. Transfer. **71**, 157 (2001).
4. R. Neu, K.B. Fournier, D. Schlogl, and J. Rice. J. Phys. B, **30**, 5057 (1997).
5. P.G. Burkhalter, C.M. Dozier, and R.D.J. Nagel. Phys. Rev. A, **15**, 700 (1977).
6. A. Zigler, H. Zmora, N. Spector, M. Klapisch, J.L. Schwob, and A. Bar-Shalom. J. Opt. Soc. Am. **70**, 129 (1980).
7. M. Klapisch, P. Mandelbaum, A. Barshalom, J.L. Schwob, A. Zigler, and S. Jackel. J. Opt. Soc. Am. **71**, 1276 (1981).
8. N. Tragin, J.P. Ghendre, P. Monier, J.C. Gauthier, C. Chenais-Popovics, J.F. Wyart, and C. Bauche-Arnoult. Phys. Scr. **37**, 72 (1988).
9. R. Radtke, C. Biedermann, J.L. Schwob, P. Mandelbaum, and R. Doron. Phys. Rev. A, **64**, 012720 (2001).
10. S.B. Utter, P. Beiersdorfer, and E. Träbert. Can. J. Phys. **80**, 1503 (2002).
11. K.B. Fournier. Atom. Data Nucl. Data Tab. **68**, 1 (1998).
12. P. Beiersdorfer, J.A. Britten, G.V. Brown, H. Chen, E.J. Clothiaux, J. Cottam, E. Forster, M.F. Gu, C.L. Harris, S.M. Kahn, J.K. Lepson, and P.A. Neill. Phys. Scr. T, **92**, 268 (2001).
13. G.V. Brown, P. Beiersdorfer, and K. Widmann. Rev. Sci. Instrum. **70**, 280 (1999).

14. S. Elliot, P. Beiersdorfer, and J. Nilsen. Phys. Scr. **49**, 556 (1994).
15. R.D. Cowan. The theory of atomic structure and spectra. University of California Press, Berkeley, Calif. USA. 1981; URL = ftp://aphysics.lanl.gov/pub/cowan.
16. U.I. Safronova, W.R. Johnson, and J.R. Albritton. Phys. Rev. A, **62**, 052505 (2000).
17. T.A. Carlson, C.W. Nestor, N. Wasserman, and J.D. McDowell. Oak Ridge National Laboratory Report. No. 4562. 1970.
18. H.V. Regemorter. Astroph. J. **136**, 906 (1962).
19. V.A. Bernshtam, Yu.V. Ralchenko, and Y. Maron. J. Phys. B, **33**, 5025 (2000).
20. V.P. Shevelko. Atoms and their spectroscopic properties. Springer-Verlag, Berlin. 1997.
21. P. Beiersdorfer, T.W. Philips, K.L. Wong, R.E. Marrs, and D.A. Vogel. Phys. Rev. A, **46**, 3812 (1992).